Perylene salts of unsymmetrical nickel and gold dithiolene complexes with 3 : 2 stoichiometry: conformational polymorphism and strong antiferromagnetic interactions

Olivier Jeannin and Marc Fourmigué*†

Received (in Montpellier, France) 14th June 2006, Accepted 29th August 2006
First published as an Advance Article on the web 12th September 2006
DOI: 10.1039/b608420f

The square-planar Au^{III} complex of the unsymmetrical tfadt dithiolate ligand (tfadt: 2-(trifluoromethyl)acrylonitrile-1,2-dithiolate) is found to exhibit conformational polymorphism in its *n*-Bu_4N^+ salt, as both *cis* and *trans* isomers were found to crystallize separately in the same crystallization batch. Electrocrystallization of perylene in the presence of the diamagnetic [*n*-Bu_4N][$Au(tfadt)_2$] or the paramagnetic ($S = 1/2$) [*n*-Bu_4N][$Ni(tfadt)_2$] nickel analog affords isostructural salts with an unusual 3 : 2 stoichiometry, that is $[Per]_3[M(tfadt)_2]_2$ (M = Au, Ni), with an alternation of dicationic $[Per]_3^{2+}$ perylene triads and dianionic $[M(tfadt)_2]_2^{2-}$ dithiolene complex dyads within one-dimensional chains. These salts are characterized by strong antiferromagnetic interactions within perylene triads and $[Ni(tfadt)_2]_2^{2-}$ dyads and an essentially diamagnetic behaviour.

Introduction

The perylene molecule has been used in the last 30 years in the preparation of molecular conductors with anions as different as halogens, simple inorganic counter ions or metal dithiolene complexes.[1] Among them, the perylene salts[2] of $M(mnt)_2^{-\bullet}$ dithiolene complexes[3] (M = Ni, Pt, Pd, Au; mnt = 1,2-dicyano-1,2-ethylenedithiolato) (Chart 1) have been extensively investigated and particularly the origin of the metal-to-insulator transition and its variations essentially depending on the nature of the metal in the dithiolene complex. It was shown for example that the Peierls transition affecting the perylene stack in $[Per]_2[Pt(mnt)_2]$ was coupled with a spin-Peierls transition on the paramagnetic $[Pt(mnt)_2]^{-\bullet}$ while the analogous salt with the diamagnetic gold complex $[Au(mnt)_2]^-$ gave a pure Peierls transition.[4] In that regard, properties of solid solutions involving both $[Pt(mnt)_2]^{-\bullet}$ and $[Au(mnt)_2]^-$ were also investigated in the $[Per]_2[Au_{1-x}Pt_x(mnt)_2]$ salts.[5] Other perylene salts with dimeric $[Fe(mnt)_2]_2$ and[6] $[Co(mnt)_2]_2$ or[7] trimeric $[Co(mnt)_2]_3^-$ moieties[8] also exhibit segregated perylene stacks. Considering the rich physics of these perylene salts with $[M(mnt)_2]^-$ dithiolene complexes, it is surprising that only a few other dithiolene complexes have been investigated in their association with perylene.

Older reports include insulating 1 : 1 complexes with $[Ni(tfd)_2]$ and $[Pt(tfd)_2]$ (tfd = 1,2-bis(trifluoromethyl)-1,2-ethylenedithiolato) which exhibit alternated stacks of neutral perylene and dithiolene complexes,[9,10] demonstrating that, with the tfd dithiolate ligand, the redox potentials of both partners disfavour the electron transfer. This drawback was circumvented using an anionic Cu^{III} dithiolene complex as $[Cu(qdt)_2]^-$ (qdt: quinoxaline-2,3-dithiolate) which is stable at the oxidation potential of perylene.[11] In this 2 : 1 $[Per]_2[Cu(qdt)_2]$ salt, perylene stacks were still observed but strongly affected by tetramerization. Another 1 : 1 salt was also described with $[Ni(Cl_4bdt)_2]^-$ (Cl_4bdt: tetrachlorobenzene-1,2-dithiolate).[12] Despite the fact that $[Ni(Cl_4bdt)_2]^-$ oxidizes at +0.73 V *vs.* SCE, that is at a lower potential than the perylene oxidation (+0.90 V *vs.* SCE), the relatively high conductivity of this semi-conducting salt was taken as an indication of a partial charge transfer, a question still open in the absence of X-ray crystal structure determination.

We have recently described[13] a novel nickel dithiolene complex based on a asymmetrically substituted dithiolate ligand, hereafter noted tfadt (tfadt: 2-(trifluoromethyl)acrylonitrile-1,2-dithiolate), which incorporates both the nitrile group of the mnt ligand and the CF_3 group of the tfd ligand. Considering the rich structural and physical properties of the perylene salts with $[M(mnt)_2]^{1-}$ anions, we decided to investigate the electrocrystallization of perylene in the presence of this paramagnetic $[Ni(tfadt)_2]^-$ complex and also extended this investigation to the still unknown, diamagnetic gold complex $[Au(tfadt)_2]^-$. We describe here the preparation, X-ray structure determination and electrochemical properties of the gold complex $[Au(tfadt)_2]^-$ in its PPh_4^+ and *n*-Bu_4N^+ salts. The electro-crystallization of the perylene donor molecule with both nickel and gold anions afforded two isostructural salts,

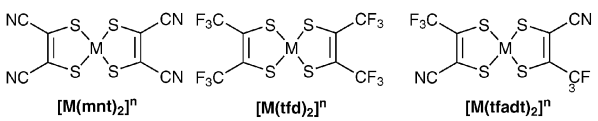

Chart 1

Laboratoire Chimie, Ingénierie Moléculaire et Matériaux (CIMMA), UMR 6200 CNRS- Université d'Angers, UFR Sciences, 2 Bd Lavoisier, 49045 Angers, France. E-mail: marc.fourmigue@univ-rennes1.fr
† Permanent address: Sciences Chimiques de Rennes, UMR 6226 CNRS-Université Rennes 1, Equipe MaCSE, Bât 10C, Campus de Beaulieu, 35042 Rennes cedex, France.

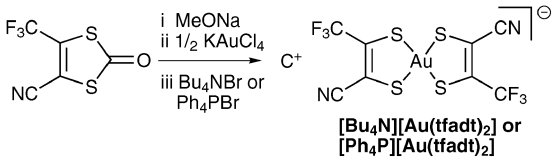

Scheme 1

which only differ by the spin state of the anion, $S = 1/2$ in the complex $[Ni(tfadt)_2]^{-\bullet}$ and $S = 0$ in $[Au(tfadt)_2]^-$. The structures of both salts and their magnetic properties will be described and compared.

Results and discussion

Synthesis

The gold complexes $(Ph_4P)[Au(tfadt)_2]$ and $(n\text{-}Bu_4N)[Au(tfadt)_2]$ were prepared (Scheme 1) as previously described[13] for the dianionic $[Ni(tfadt)_2]^{2-}$ nickel complex from the corresponding 4-cyano-5-trifluoromethyl-1,3-dithiol-2-one[14] by treatment with MeONa in MeOH, addition of $KAuCl_4$ and precipitation as Ph_4P^+ or $(n\text{-}Bu)_4N^+$ salt by addition in a solution of Ph_4PBr or $(n\text{-}Bu)_4NBr$, respectively.

Recrystallization of the PPh_4^+ salt afforded green crystals while the recrystallization of the $(n\text{-}Bu)_4N^+$ salt by slow evaporation of a MeOH solution afforded a mixture of green prisms and brown plates, identified from the X-ray diffraction studies as the *cis* and *trans* isomers, respectively (see Scheme 2).

Variable temperature (VT) NMR studies were performed on this salt in order to evaluate the activation energy for a possible *cis–trans* isomerism in solution, by analogy with similar studies performed on the diamagnetic $[Ni(tfadt)_2]^{2-}$ nickel complex.[13] In the latter indeed, the two isomers were identified on ^{19}F NMR spectra below 260 K (coalescence temperature) with an associated activation energy $\Delta G^{\#}$ of 52.6 kJ mol^{-1}. Similar ^{19}F NMR experiments performed on $[n\text{-}Bu_4N][Au(tfadt)_2]$ show the presence of one single resonance from room temperature down to 200 K in CH_2Cl_2, demonstrating that in the same conditions, the gold complex equilibrates between both isomers at a faster rate than the nickel complex, the probable consequence of a lower associated activation energy.

Cyclic voltammetry experiments conducted in CH_2Cl_2 (Fig. 1) shows the presence of two reversible redox waves, one in reduction at $E_{1/2} = -1.35$ V *vs.* Fc^+/Fc, attributable to the $[Au(tfadt)_2]^{2-}/[Au(tfadt)_2]^{1-}$ process while the wave observed in oxidation at $E_{1/2} = +0.745$ V *vs.* Fc^+/Fc corresponds to the $[Au(tfadt)_2]^{1-}/[Au(tfadt)_2]^{0}$ redox process. Values of the corresponding symmetrical $[Au(mnt)_2]$ and $[Au(tfd)_2]$ complexes have been also collected in Table 1 for comparison, showing

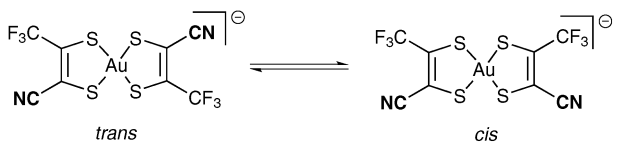

Scheme 2

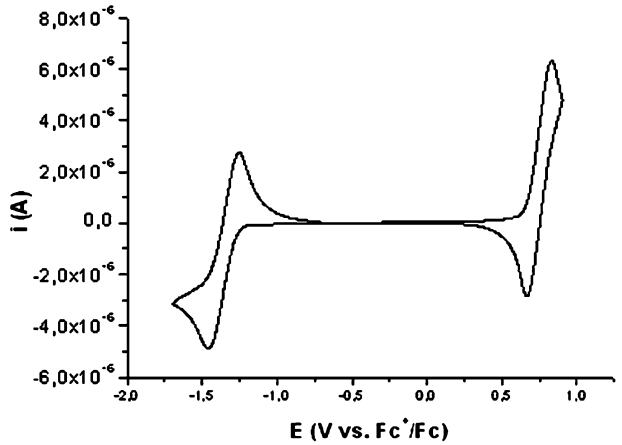

Fig. 1 Cyclic voltammetry of the gold complex $[(n\text{-}Bu)_4N][Au(tfadt)_2]$.

that the tfadt ligand exhibits a behaviour close to that of the mnt and tfd ligands.

Structural determinations

$[Ph_4P][Au(tfadt)_2]$ crystallizes in the monoclinic system, space group $C2/c$, with the Ph_4P^+ cation located on a two-fold axis and the $[Au(tfadt)_2]^-$ on an inversion center, thus with a *trans* configuration relative to the CN and CF_3 groups. The CF_3 group is further disordered on two positions related to each other by a 60° rotation. This salt is actually isostructural with the analogous nickel complex $[Ph_4P][Ni(tfadt)_2]$.[13] On the other hand, both kinds of crystals isolated from the recrystallization of $[n\text{-}Bu_4N][Au(tfadt)_2]$ were found to crystallize in the triclinic system, space group $P\bar{1}$, with both cation and anion in general position in the unit cell. The brown crystals were identified as the *trans* isomer (Fig. 2) while the green crystals are the *cis* isomer (Fig. 3). Bond lengths and angles within the metallacycles are collected in Table 2 for comparison. Note the differences between the C–S bond lengths (*b* and *b′*), depending on the nature of the substituent (–CN or $–CF_3$) on the carbon, a consequence of the unsymmetrical nature of the dithiolate ligand. This shortening of the $(F_3C–)C–S$ bond (*b′*) relative to the (NC–)C–S bond (b) was observed in the nickel complexes and, as shown in the scheme of Table 2, is attributed to an unsymmetrical mesomeric form due to the more strongly withdrawing effect of the –CN moiety when compared with the $–CF_3$ one.

It is also important to note here that the isolation of a square-planar dithiolene complex in its *cis* form is highly unexpected. Indeed, considering the few described examples

Table 1 Cyclic voltammetry data, *vs.* Fc^+/Fc. Values in parentheses are original data reported *vs.* SCE. For comparison purposes, a correction of −0.40 V has been applied to generate potentials *vs.* Fc^+/Fc

Compound	$E_{1/2}(-2/-1)$	$E(-1/0)$	Solvent	Ref.
$[Au(mnt)_2]^{-2,-1,0}$	−1.33 (−0.93)	+0.70 (1.10)	CH_2Cl_2	15
$[Au(tfadt)_2]^{-2,-1,0}$	−1.35	+0.745	CH_2Cl_2	This work
$[Au(tfd)_2]^{-2,-1,0}$	−1.37 (−0.97)	+0.92 (1.32)	CH_2Cl_2	16

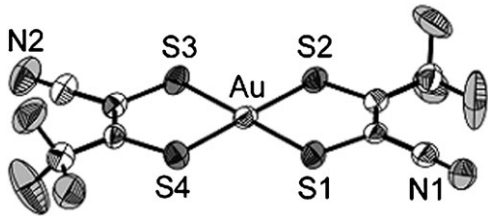

Fig. 2 ORTEP view (at 50% probability level) of the *trans*-$[Au(tfadt)_2]^-$ species as its $(n\text{-}Bu)_4^+$ salt.

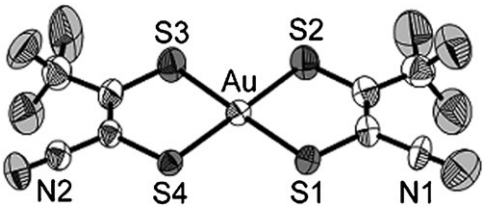

Fig. 3 ORTEP view (at 50% probability level) of the *cis*-$[Au(tfadt)_2]^-$ species as its $(n\text{-}Bu)_4^+$ salt.

of square planar dithiolene complexes involving asymmetrically substituted 1,2-dithiolate ligands and crystallographically characterized (Chart 2), as $[Ni(adt)_2]^{2-,1-}$,[17,18] $[Ni(dmt)_2]^-$,[19] the fused thiophene derivatives $[Au(dtpdt)_2]^-$ or[20] $[M(\alpha\text{-}tpdt)_2]^-$ with M = Ni,[21] Co,[22] Pt,[22] the phenyl dithiolate $[Ni(sdt)_2]$,[23] or their pyridine analogs $[Au(3\text{-}pedt)_2]^-$, $[Au(4\text{-}pedt)_2]^-$,[24] they all are found to crystallize in the *trans* form, except two, $[Au(sdt)_2]^-$ and $[Au(2\text{-}pedt)_2]^-$, which were very recently described to crystallize in the *cis* form, in their PPh_4^+ salts.[24]

Earlier DFT calculations[13] performed on the *cis*- and *trans*-isomers of the nickel $[Ni(tfadt)_2]^{2-,1-}$ had shown that the energy difference between both isomers was negligible. It is probably also the case here for the gold complex. However, the fact that we can isolate both isomers in the same crystallization batch demonstrates not only that the molecular *cis* and *trans* structures are very close in energy and that they interconvert easily (*cf.* VT NMR data) but also that the solid state structures have essentially the same energy under the crystallization conditions used here. This form of polymorphism has been described as conformational polymorphism,[25] where a molecule adopts significantly different conformations in different crystal polymorphs. McCrone's criterion[26] is that polymorphs are different in crystal structure but identical in the liquid or vapor states. This implies that crystals containing molecules with different atomic arrangements are to be classed as polymorphs if the molecules concerned interconvert rapidly in the melt or in solution to give the same equilibrium mixture. This is indeed the case here in $[Au(tfadt)_2]^-$, as demonstrated from the VT NMR studies. This salt represents to our knowledge the very first example of reported simultaneous crystallization of both *cis* and *trans* isomers.

In the crystal, the anions adopt very different solid state organizations. Indeed, in the *cis* isomer (Fig. 4), the complex anions form chains running along *c*, separated from each other by the bulky $n\text{-}Bu_4N^+$ cations and characterized by lateral intermolecular S···S van der Waals interactions.

On the other hand, as shown in Fig. 5, the *trans* complex adopts a dimeric structure with an intermolecular Au···Au distance at 4.13 Å, the shortest S···S distances in 4.11–4.13 Å range and Au···S distances at 3.86 Å. These short Au···S interactions are probably at the origin of this dimer formation and drive its crystallization, since it is not isostructural with the isosteric nickel $[n\text{-}Bu_4N][trans\text{-}Ni(tfadt)_2]$ complex.

Perylene salts

Electrocrystallization experiments were performed with perylene in the presence of either the paramagnetic $[(n\text{-}Bu)_4N][Ni(tfadt)_2]$ or the analogous diamagnetic $[(n\text{-}Bu)_4N][Au(tfadt)_2]$ complex. Crystals were harvested on the anode and structurally and magnetically characterized. X-Ray crystal structure determinations showed that both salts are isostructural and can be formulated as $[Per]_3[M(tfadt)_2]_2$ (M = Ni, Au), that is a highly unusual 3 : 2 stoichiometry. They crystallize in the triclinic system, space group $P\bar{1}$ with one perylene on an inversion center, one other perylene and a dithiolene complex in general position in the unit cell. In both

Table 2 Bond lengths within the metallacycle in the gold dithiolene complexes

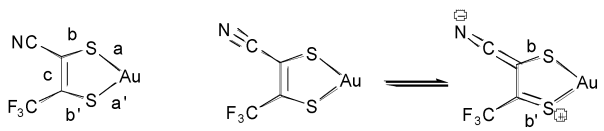

	a	*a′*	*b*	*b′*	*c*
trans-$[Au(tfadt)_2]^{-a}$	2.2948(16)	2.2848(15)	1.742(6)	1.720(6)	1.336(7)
trans-$[Au(tfadt)_2]^{-b}$	2.306(2)	2.305(2)	1.747(8)	1.743(7)	1.350(10)
	2.307(2)	2.314(2)	1.755(8)	1.745(7)	1.332(10)
trans-$[Au(tfadt)_2]^{-c}$	2.304(1)	2.302(1)	1.753(5)	1.734(4)	1.341(6)
	2.305(1)	2.305(1)	1.754(5)	1.738(4)	1.340(6)
cis-$[Au(tfadt)_2]^{-b}$	2.2933(16)	2.3045(19)	1.764(6)	1.730(7)	1.326(9)
	2.3120(14)	2.3132(15)	1.760(5)	1.730(7)	1.340(9)

[a] As its Ph_4P^+ salt. [b] As its $(n\text{-}Bu)_4N^+$ salt. [c] As its perylene salt.

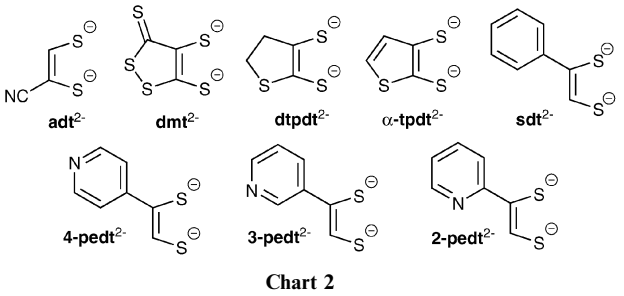

Chart 2

salts, the dithiolene complex adopts a *trans* conformation, with one of the two CF_3 groups affected by disorder. In the solid state (Fig. 6), the perylene molecules associate into inversion-centred triads, alternating with inversion-centred metal dithiolene dyads into stacks $\cdots$[Per]$_3$[M(tfadt)$_2$]$_2$ [Per]$_3$[M(tfadt)$_2$]$_2\cdots$ running along the [1 0 −1] direction.

Such a stoichiometry with trimeric perylene units is rather unusual and the only comparable system described so far is based on an modified perylene, the perylo[1,12-*bcd*]thiophene (pet, Chart 3) which exhibits with [Ni(mnt)$_2$]$^{-\bullet}$ the same stoichiometry, that is [pet]$_3$[Ni(mnt)$_2$]$_2$.[27] In this salt however, the solid state organization strongly differs as segregated stacks of anions and cations are observed, with trimerized pet chains alternating with strongly dimerized [Ni(mnt)$_2$] chains.

One important point to be addressed here is the actual electronic state of the perylene and the [M(tfadt)$_2$] moieties in both salts. Indeed, the 1 : 1 tfd salts, that is [Per][Ni(tfd)$_2$], are known to be neutral insulators while most salts with [M(mnt)$_2$]$^-$ are mixed-valence conducting salts, with the exception of a 1 : 1 [Per][Pt(mnt)$_2$] salt.[28] The [Ni(tfadt)$_2$]$^{-\bullet}$ is known to oxidize reversibly to the neutral complex at 0.51 V *vs.* Fc$^+$/Fc while [Au(tfadt)$_2$]$^-$ oxidizes at a notably higher potential, 0.745 V *vs.* Fc$^+$/Fc. We should therefore compare those values with the oxidation potential of perylene itself in order to determine if the dithiolene complexes might eventually oxidize below perylene. The latter oxidizes at 0.90 V *vs.* SCE, that is around 0.50 V *vs.* Fc$^+$/Fc and thus close but below the oxidation potentials of both Ni and Au tfadt complexes. It is therefore expected that during the electrocrystallization experiments, the perylene is oxidized rather than the dithiolene complexes. Furthermore, analysis of the bond lengths within the [Ni(tfadt)$_2$] complex, as a monoanion in its (n-Bu)$_4$N$^+$ or PPh$_4^+$ salt (Table 3) shows that the

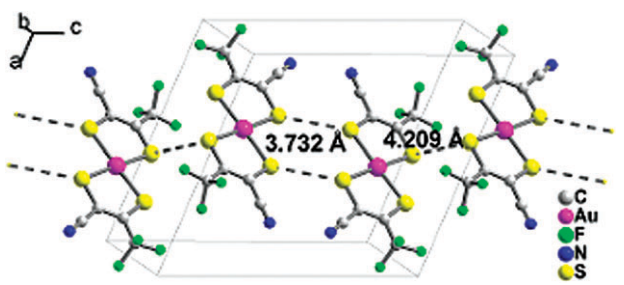

Fig. 4 A view of the unit cell of [n-Bu$_4$N][*cis*-Au(tfadt)$_2$]. The n-Bu$_4^+$ cations have been omitted for clarity.

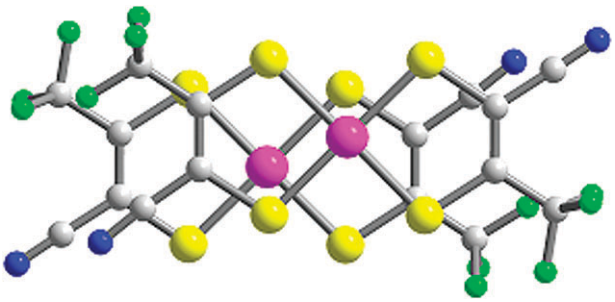

Fig. 5 A projection view (perpendicular to the molecular planes) of the dimeric entities [Au(tfadt)$_2$]$_2^{2-}$ in [n-Bu$_4$N][*trans*-Au(tfadt)$_2$].

monoanionic state is indeed the actual oxidation state in [Per]$_3$[Ni(tfadt)$_2$]$_2$, affording the very same formulation as with the gold complex, that is [Per]$_3^{2+}$[Ni(tfadt)$_2$]$^{2-}$. The question then arises of the magnetic state of both dicationic and dianionic moieties in these salts.

The temperature dependence of the magnetic susceptibility was determined on both salts from SQUID measurements on polycrystalline samples. As shown in Fig. 7, the gold salt is essentially diamagnetic with a negligible Curie tail at the lowest temperatures corresponding to 0.6% $S = 1/2$ magnetic defects. The nickel complex also exhibits a Curie type behaviour but with a Curie constant corresponding to about 9% of a $S = 1/2$ species. Tacking into account the $S = 0$ state of the [Au(tfadt)$_2$]$^-$ gold dithiolene complex, the diamagnetic character of its perylene salt unambiguously demonstrates that the dicationic [Per]$_3^{2+}$ trimer is also in a singlet ground state at room temperature and below. As a consequence, the weak magnetic contribution in the nickel salt can only arise from the [Ni(tfadt)$_2$]$^{-\bullet}$ complex.

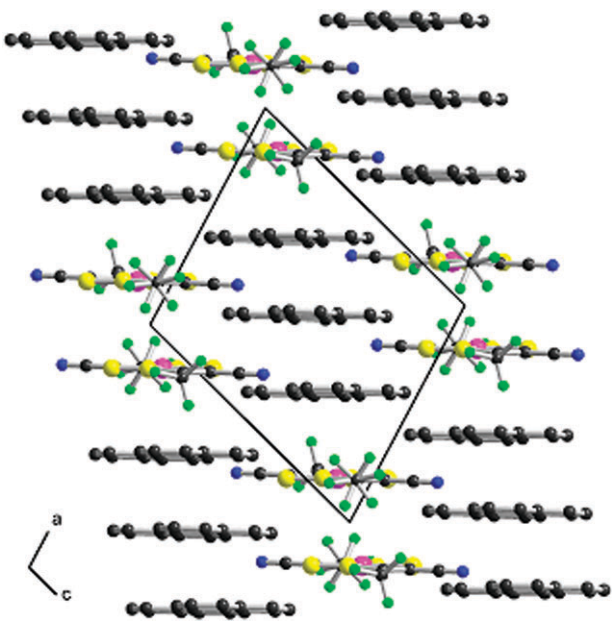

Fig. 6 A projection view of one (*a*,*c*) layer showing the perylene triads and metal dithiolene dyads. The two disordered positions of one CF_3 groups are shown.

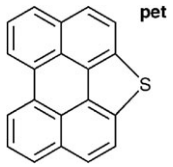

Chart 3

Despite the isostructural character of both salts, slight structural differences are observed within the inorganic dyads and organic triads. The most spectacular one is shown in Fig. 8: the diamagnetic $[Au(tfadt)_2]^-$ complex exhibits an overlap with lateral offset together with intermolecular Au···Au distance at 3.98 Å, a structure close to that described above in its *n*-Bu_4N^+ salt (Fig. 5). On the other hand, with the radical $[Ni(tfadt)_2]^{-\bullet}$ nickel complex, the metal dithiolene dyads adopt an almost perfectly eclipsed configuration. Indeed, the shortest S···S intermolecular contacts are found at 3.662 and 3.740 Å within the $[Ni(tfadt)_2]_2$ dyads while they exceed 3.979 and 4.031 Å in the gold $[Au(tfadt)_2]_2$ dyads. Similarly, the plane-to-plane distances amount to 3.632(5) Å in $[Ni(tfadt)_2]_2$ dyads and 3.822(3) Å in $[Au(tfadt)_2]_2$ dyads.

These features are clearly the consequence of the radical nature of the nickel $[Ni(tfadt)_2]^{-\bullet}$ complex. The interaction between the singly occupied molecular orbitals of both $[Ni(tfadt)_2]^{-\bullet}$ moieties leads to a bonding and antibonding combinations which can be characterized by the calculation of the interaction energy, $\beta_{ij} = \langle\varphi_i|H_{\text{eff}}|\varphi_j\rangle$, where φ_i and φ_j are the relevant frontier orbitals of each pair of neighbour complexes.[29] The calculated interaction energy $\beta_{\text{Ni–Ni}}$ within the nickel dyad amounts to 0.409 eV, a value associated with very strong coupling. The magnetic susceptibility of such a singlet–triplet system is described by the Bleaney–Bower equation (eqn (1)) where J is the energy gap between the singlet and triplet state, N_A is Avogadro's number, g the Landé factor, μ_B the Bohr magneton, k_B the Boltzmann constant and T the absolute temperature.[30]

$$\chi_{ST} = \frac{2N_A g^2 \mu_B^2}{k_B T} \frac{1}{3 + \exp(-J/k_B T)} \qquad (1)$$

In a Hubbard model, the relationship between the interaction parameter J and the calculated interaction energy β_{ij} can be written as $J = \frac{\beta^2}{U}$, where U is the on-site Coulomb repulsion, which amounts to ~1 eV in most molecular materials. Accordingly, the calculated 0.409 eV value for $\beta_{\text{Ni–Ni}}$ corresponds to a very large $J_{\text{Ni–Ni}}/k_B$ value of 1856 K. As a consequence, the triplet state of the nickel complex dyad will be essentially unoccupied at room temperature or below and should not contribute to the magnetic susceptibility.

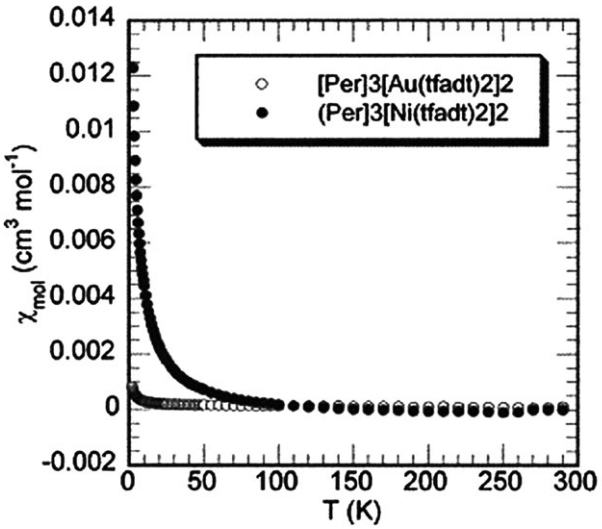

Fig. 7 Temperature dependence of the magnetic susceptibility of $[Per]_3[M(tfadt)_2]_2$, M = Au, Ni.

The interaction between perylene molecules develops within triads, with one perylene on an inversion center, flanked by two perylene molecules corresponding to each other by the same inversion center. The overlap between the centrosymmetric central molecule and one other perylene molecule is shown in Fig. 9 for both compounds. We observe a lateral offset in both salts, together with a noticeable longitudinal shift only in the salt of the gold complex. The centrosymmetric and an neighbour perylene molecules are almost parallel, with an angle between the molecular mean planes of 0.40(4)° in the nickel complex salt and 0.69(4)° in the gold complex salt and an averaged plane-to-plane distance of 3.36–3.37 Å. The corresponding calculated overlap interaction energy $\beta_{\text{Per–Per}}$ amounts to 0.362 eV in the nickel complex salt, which would correspond to a $J_{\text{Per–Per}}/k_B$ evaluated at 1520 K. Accordingly,

Table 3 Bond lengths within the metallacycle in the nickel tfadt complexes

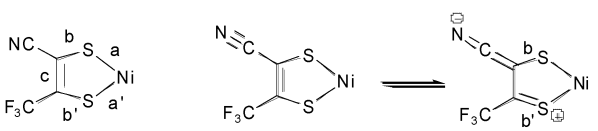

	a	*a′*	*b*	*b′*	*c*	Ref
$[Ni(tfadt)_2]^{2-a}$	2.167	2.170	1.745	1.729	1.356	13
$[Ni(tfadt)_2]^{-a}$	2.139	2.140	1.726	1.704	1.358	13
$[Ni(tfadt)_2]^{-b}$	2.137(2)	2.138(2)	1.740(5)	1.706(5)	1.339(7)	This work
	2.140(2)	2.143(2)	1.733(5)	1.711(5)	1.327(7)	

[a] Averaged values from the $(n\text{-Bu})_4N^+$ and PPh_4^+ salts. [b] In its perylene salt.

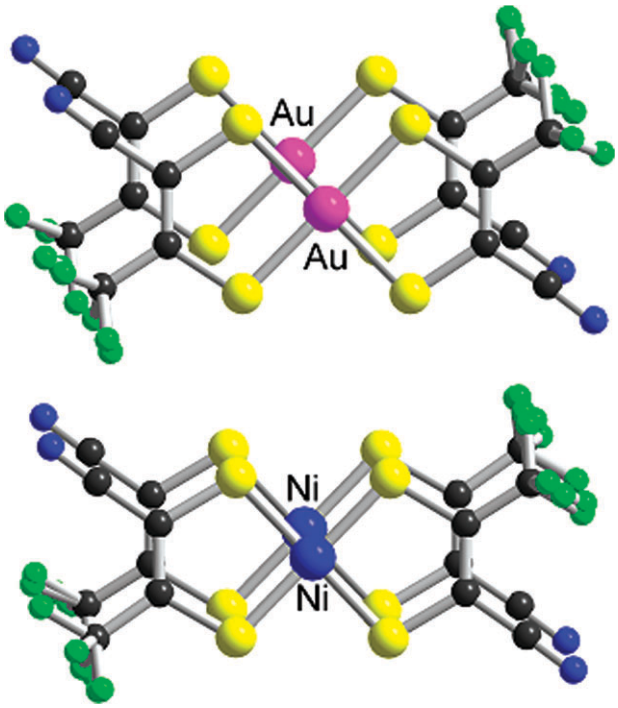

Fig. 8 A view of the overlap between $[M(tfadt)_2]^{-\bullet}$ within the dyads in $[Per]_3[M(tfadt)_2]_2$, M = Au (top) or Ni (bottom). The two orientations of the disordered CF_3 group have been shown.

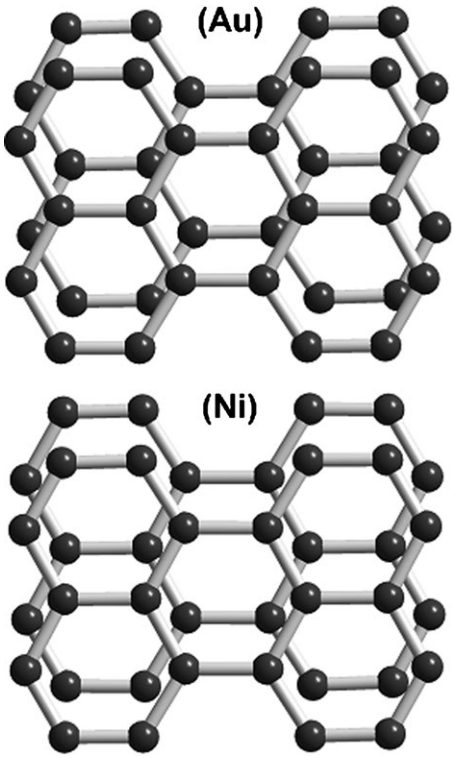

Fig. 9 A view of the overlap between perylene molecules within the triads in $[Per]_3[M(tfadt)_2]_2$, M = Au (top) and Ni (bottom).

the dicationic perylene triad is also expected to be diamagnetic, as indeed experimentally observed in the gold complex salt. The weak Curie–Weiss paramagnetism observed in the nickel salt most probably arises from non-interacting paramagnetic $[Ni(tfadt)_2]^-$ defects.

Conclusion

Square-planar complexes of unsymmetrical dithiolate ligands such as (tfadt: 2–(trifluoromethyl)acrylonitrile-1,2-dithiolate) are found to exhibit conformational polymorphism in the *n*-Bu_4N^+ salt, as both *cis* and *trans* isomers were found to crystallize separately in the same crystallization batch. Electrocrystallization of perylene in the presence of the diamagnetic [*n*-Bu_4N][Au(tfadt)$_2$] or the paramagnetic (S = 1/2) [*n*-Bu_4N][Ni(tfadt)$_2$] nickel analogue affords isostructural salts with an unusual 3 : 2 stoichiometry, that is $[Per]_3[M(tfadt)_2]_2$ (M = Au, Ni), with an alternation of dicationic $[Per]_3^{2+}$ perylene triads and dianionic $[M(tfadt)_2]_2^{2-}$ dithiolene complex dyads within one-dimensional chains. These salts are characterized by strong antiferromagnetic interactions within perylene triads and $[Ni(tfadt)_2]_2^{2-}$ dyads and an essentially diamagnetic behaviour.

Experimental

Syntheses

The nickel complex (*n*-Bu_4N)[Ni(tfadt)$_2$] and 4-cyano-5-trifluoromethyl-1,3-dithiol-2-one were prepared as previously described. MeOH was dried by refluxing on Mg and distillation prior to use.

[*n*-Bu_4N][Au(tfadt)$_2$]

4-Cyano-5-trifluoromethyl-1,3-dithiol-2-one (0.6 g, 2.64 mmol) was added to a solution of Na (0.15 g, 6.52 mmol) in dist. MeOH (10 mL). After stirring for 45 min, $KAuCl_4$ (0.5 g, 1.32 mmol) was added and the mixture was stirred overnight. *n*-Bu_4NBr (0.72 g, 2.23 mmol) was then added to the solution, followed by distilled water (50 mL). The precipitate was filtered, washed with water and Et_2O (5 mL) to yield the title compound (0.41 g, 55%) as a green powder. Crystallization by slow evaporation of a MeOH solution yielded a mixture of green prisms and brown plates. MALDI-TOF-MS: Calc. 562.85; Found. 562.83. Anal. Calcd for $C_{24}H_{36}F_6N_3AuS_4$: C, 35.77; H, 4.50; N, 5.21. Found: C, 35.57; H, 4.37 N, 5.24%. IR (KBr) ν (cm^{-1}): 2211.5 (C≡N).

[Ph_4P][Au(tfadt)$_2$]

4-Cyano-5-trifluoromethyl-1,3-dithiol-2-one (0.9 g, 4.26 mmol) was added to a solution of Na (0.3 g, 13 mmol) in dist. MeOH (10 mL). After stirring for 45 min, $KAuCl_4$ (1.02 g, 2.24 mmol) was added, the mixture stirred for 1 h and Ph_4PBr (0.95 g, 2.26 mmol) was added. After stirring overnight, the precipitate was filtered, dissolved hot in CH_3CN and filtered again. After cooling, the green brown precipitate was filtered and washed with Et_2O. Diffusion of pentane into an acetone solution yielded the salt (1.2 g, 62%) as of green elongated plates. Anal. Calcd for $C_{32}H_{20}F_6N_2AuS_4P$: C, 42.58; H, 2.23; N, 3.10. Found: C, 42.54; H, 2.23 N, 3.02%.

Table 4 Crystallographic data

Compound	$(PPh_4)[Au(tfadt)_2]$	*trans* $(n\text{-}Bu_4N)$ $[Au(tfadt)_2]$	*cis* $(n\text{-}Bu_4N)$ $[Au(tfadt)_2]$	$[Per]_3$ $[Ni(tfadt)_2]_2$	$[Per]_3$ $[Au(tfadt)_2]_2$
Formula	$C_{32}H_{20}AuF_6N_2PS_4$	$C_{24}H_{36}AuF_6N_3S_4$	$C_{24}H_{36}AuF_6N_3S_4$	$C_{38}H_{18}F_6N_2NiS_4$	$C_{38}H_{18}F_6N_2AuS_4$
Fw	902.68	805.76	805.76	803.49	941.79
Cryst. system	Monoclinic	Triclinic	Triclinic	Triclinic	Triclinic
Space group	$C2/c$	$P\bar{1}$	$P\bar{1}$	$P\bar{1}$	$P\bar{1}$
a/Å	25.7658(12)	11.1550(13)	11.5030(12)	10.8853(14)	10.8670(13)
b/Å	8.0568(5)	11.7052(13)	12.2691(14)	12.6566(14)	12.7568(16)
c/Å	17.6766(9)	13.5301(15)	12.5077(14)	13.1882(16)	13.2210(15)
α/deg	—	73.117(13)	104.268(13)	113.253(13)	111.176(13)
β/deg	117.347(4)	78.734(14)	113.245(12)	103.614(14)	103.135(14)
γ/deg	—	67.536(13)	92.870(12)	94.149(14)	96.571(15)
V/Å^3	3259.4(3)	1555.1(3)	1550.2(3)	1594.4(3)	1624.9(3)
Z	4	2	2	2	2
D_{calc}/Mg m^{-3}	1.840	1.721	1.726	1.674	1.925
Diffractometer	Kappa-CCD	Stoe-IPDS	Stoe-IPDS	Stoe-IPDS	Stoe-IPDS
T/K	293(2)	293(2)	293(2)	293(2)	293(2)
μ/mm^{-1}	4.880	5.054	5.069	0.94	4.853
θ-range/deg	2.38–27.52	1.94–25.87	1.85–25.97	1.78–25.99	1.97–25.94
Meas. reflns	11788	15016	14990	15531	15849
Indep. reflns	3728	5563	5543	5735	5865
R_{int}	0.0295	0.0641	0.0323	0.0516	0.0394
$I > 2\sigma(I)$ reflns	2700	4285	4711	2597	4750
Abs. corr.	Empirical	Gaussian	Gaussian	Gaussian	Gaussian
T_{max}, T_{min}	1.0, 0.6334	0.8603, 0.2489	0.5580, 0.2872	0.9650, 0.6801	0.8153, 0.1486
Refined par.	238	343	343	515	487
$R(F), I > 2\sigma(I)$	0.0397	0.0385	0.0334	0.046	0.0258
$wR(F^2)$, all	0.1187	0.0946	0.0879	0.1385	0.0499
$\Delta\rho$ (e Å^{-3})	+1.75, −1.29	+1.15,−1.74	+1.60, −1.24	+0.57, −0.52	+0.56, −0.50

$[Per]_3[Ni(tfadt)_2]_2$

A solution of $(n\text{-}Bu_4N)[Ni(tfadt)_2]$ (33 mg) in CH_2Cl_2 (15 mL) was shared in a two-compartment cell divided by a glass frit while perylene (20 mg) was added to the anodic compartment. A 1 μA current was applied for two weeks giving black plates on the anode. IR (KBr) ν (cm^{-1}): 2207.64 (C≡N).

$[Per]_3[Au(tfadt)_2]_2$

A solution of $(n\text{-}Bu_4N)[Au(tfadt)_2]$ (20 mg) in a mixture of dist. CH_2Cl_2 (9 mL) and CH_3CN (3 mL) was shared in a two-compartment cell divided by a glass frit while perylene (10 mg) was added to the anodic compartment. A 0.5μA current was applied for two weeks giving black hexagonal plates on the anode. IR (KBr) ν (cm^{-1}): 2211.5 (C≡N).

Electrochemistry

Cyclic voltammetry was performed in CH_2Cl_2 containing $n\text{-}Bu_4NPF_6$ 0.05 M as electrolyte. A platinum disk and platinum wire were used as working and counter electrode respectively together with an Ag^+/Ag reference. Ferrocene was added at the end of the experiment.

Crystallography‡

Crystals were mounted at the end of a glass fiber with Araldite™ glue. Data were collected on a Stoe Imaging Plate Diffraction System (IPDS) with graphite monochromated Mo-Kα radiation (λ = 0.710 73 Å). The crystal data are summarized in Table 4. Structures were solved by direct methods (SHELXS-97) and refined (SHELXL-97) by full matrix least-squares methods. Numerical absorption corrections were applied for all structures. Hydrogen atoms were introduced at calculated positions (riding model), included in structure factor calculations, and not refined. Disorder models on the CF_3 groups had to be applied in both perylene salts, affecting strongly one of the CF_3 groups in both Ni and Au complexes with two sets of 50 : 50 occupation parameters, rotated from each other by 60° in the Au complex, by ∼45° in the Ni complex. The second CF_3 group of the Ni complex was also separated into two equal contributions, differing by a rotation of a few degrees only.

‡ CCDC reference numbers 616047–616051. For crystallographic data in CIF or other electronic format see DOI: 10.1039/b608420f

Magnetic measurements

Magnetic susceptibility measurements were performed on a Quantum Design MPMS-2 SQUID magnetometer operating on the range 2–300 K at 5000 G with polycrystalline samples. Gelatin capsules were used with a magnetization contribution of $-2.37\ 10^{-6} + (2.2\ 10^{-6}/(T + 2))$ emu G g^{-1} which was used for correction of the experimental magnetization. Molar susceptibilities were then corrected for Pascal diamagnetism.

Acknowledgements

We thank Ph. Molinié (Institut Jean Rouxel, Nantes, France) for giving us access to the SQUID magnetometer. This work was supported by the CNRS, and by the Ministry of Education and Research (France) through a PhD grant (to O. J.).

References

1 For a review, see: M. Almeida, R. T. Henriques, in *Handbook of Organic Conductive Molecules and Polymers*, ed. H. S. Nalwa, John Wiley and Sons, Chichester, 1997, vol. 1, ch. 2, p. 87.

2 V. Gama, M. Almeida, R. T. Henriques, I. C. Santos, A. Domingos, S. Ravy and J.-P. Pouget, *J. Phys. Chem.*, 1991, **95**, 4263.
3 N. Robertson and L. Cronin, *Coord. Chem. Rev.*, 2002, **227**, 93.
4 (*a*) A. Matos, G. Bonfait, R. T. Henriques and M. Almeida, *Phys. Rev. B*, 1996, **54**, 15307; (*b*) G. Bonfait, M. J. Matos, R. T. Henriques and M. Almeida, *Physica B (Amsterdam)*, 1995, **211**, 297; (*c*) A. Domingos, R. T. Henriques, V. Gama, M. Almeida, A. Vieira and L. Alcacer, *Synth. Met.*, 1989, **27B**, 411.
5 (*a*) M. J. Matos, V. Gama, G. Bonfait and R. T. Henriques, *Synth. Met.*, 1993, **56**, 1858; (*b*) K. Monchi, M. Poirier, C. Bourbonnais, M. J. Matos and R. T. Henriques, *Synth. Met.*, 1999, **103**, 2228.
6 (*a*) V. Gama, R. T. Henriques, M. Almeida, C. Bourbonnais, J.-P. Pouget, D. Jérome, P. Auban-Senzier and B. Gotschy, *J. Phys. I*, 1993, **3**, 1235; (*b*) V. Gama, R. T. Henriques, G. Bonfait, L. C. Pereira, J. Waerenborgh, I. C. Santos, M. T. Duarte, J. M. P. Cabral and M. Almeida, *Inorg. Chem.*, 1992, **31**, 2598.
7 (*a*) L. F. Veiros, M. J. Calhorda and E. Canadell, *Inorg. Chem.*, 1994, **33**, 4290; (*b*) V. Gama, R. T. Henriques, G. Bonfait, M. Almeida, A. Meetsma, S. Vansmaalen and J. L. Deboer, *J. Am. Chem. Soc.*, 1992, **114**, 1986.
8 V. Gama, R. T. Henriques, M. Almeida, L. Veiros, M. J. Calhorda, A. Meetsma and J. L. De Boer, *Inorg. Chem.*, 1993, **32**, 3705.
9 R. D. Schmitt, R. M. Wing and A. H. Maki, *J. Am. Chem. Soc.*, 1969, **91**, 4394.
10 R. C. Wheland and J. L. Gillson, *J. Am. Chem. Soc.*, 1976, **98**, 3916.
11 I. C. Santos, J. A. Ayllon, R. T. Henriques, M. Almeida, L. Alcacer and M. T. Duarte, *Acta Crystallogr., Sect. C*, 1997, **53**, 1768.
12 L. L. Gonçalves, V. Gama, R. T. Henriques and M. Almeida, *Synth. Met.*, 1991, **40**, 397.
13 O. Jeannin, J. Delaunay, F. Barrière and M. Fourmigué, *Inorg. Chem.*, 2005, **44**, 9763.
14 O. Jeannin and M. Fourmigué, *Chem.–Eur. J.*, 2006, **12**, 2994.
15 J. C. Fitzmaurice, A. M. Z. Slawin, D. J. Williams, J. D. Woolins and A. J. Lindsay, *Polyhedron*, 1990, **9**, 1561.
16 A. L. Balch, I. G. Dance and R. H. Holm, *J. Am. Chem. Soc.*, 1968, **90**, 1139.
17 M. Fourmigué and J. N. Bertran, *Chem. Commun.*, 2000, 2111.
18 L. N. Dawe, L. Turnbow, J. M. Miglioi, M. L. Taliaferro, W. W. Shum, J. D. Bagnato, L. N. Zakharov, A. L. Rheingold, A. M. Arif, M. Fourmigué and J. S. Miller, *Inorg. Chem.*, 2005, **44**, 7530.
19 O. Lindqvist, L. Sjolin, J. Sieler, G. Steimecke and E. Hoyer, *Acta Chem. Scand. A*, 1982, **36**, 853.
20 D. Belo, H. Alves, E. B. Lopes, M. T. Duarte, V. Gama, R. T. Henriques, M. Almeida, A. Pérez-Benítez, C. Rovira and J. Veciana, *Chem.–Eur. J.*, 2001, **7**, 511.
21 D. Belo, H. Alves, S. Rabaça, L. C. Pereira, M. T. Duarte, V. Gama, R. T. Henriques, M. Almeida, E. Ribera, C. Rovira and J. Veciana, *Eur. J. Inorg. Chem.*, 2001, 3127.
22 D. Belo, M. J. Figueira, J. Mendonça, I. C. Santos, M. Almeida, R. T. Henriques, M. T. Duarte, C. Rovira and J. Veciana, *Eur. J. Inorg. Chem.*, 2005, 3327.
23 A. Sugimori, N. Tachiya, M. Kajitani and T. Akiyama, *Organometallics*, 1996, **15**, 5664.
24 J. M. Tunney, A. J. Blake, E. S. Davies, J. McMaster, C. Wilson and C. D. Garner, *Polyhedron*, 2006, **25**, 591.
25 J. Bernstein and A. T. Hagler, *J. Am. Chem. Soc.*, 1978, **100**, 673.
26 W. C. McCrone, *Polymorphism in Physics and Chemistry of the Organic Solid State*, ed. D. Fox, M. M. Labes and A. Weissberger, Interscience, New York, 1965, vol. 11, pp. 726–767.
27 J. Morgado, I. C. Santos, L. F. Veiros, R. T. Henriques, M. Duarte, M. Almeida and L. Alcacer, *J. Mater. Chem.*, 1997, **7**, 2387.
28 R. P. Shibaeva, V. F. Kaminskii, M. A. Simonov, E. B. Yagubskii and E. E. Kostyuchenko, *Kristallografiya (Crystallogr. Rep.)*, 1985, **30**, 488.
29 (*a*) M. H. Whangbo, J. M. Williams, P. C. W. Leung, M. A. Beno, T. J. Emge and H. H. Wang, *Inorg. Chem.*, 1985, **24**, 3500; (*b*) M. H. Whangbo, J. M. Williams, P. C. W. Leung, M. A. Beno, T. J. Emge, H. H. Wang, K. D. Carlson and G. W. Crabtree, *J. Am. Chem. Soc.*, 1985, **107**, 5815.
30 O. Kahn, *Molecular Magnetism*, VCH, Weinheim, 1993.